



One-dimensional manganese(III) and iron(III) coordination polymers assembled by N₂O₂-donor Schiff bases and 4,4'-bipyridine: syntheses, structures and properties

ANKIT KUMAR SRIVASTAVA, SUPRIYA MONDAL and SAMUDRANIL PAL*

School of Chemistry, University of Hyderabad, Hyderabad 500 046, India

E-mail: spal@uohyd.ac.in

Dedicated to Professor Bhaskar G. Mayia.

MS received 15 April 2021; revised 4 May 2021; accepted 8 May 2021

Abstract. Reactions of Mn(ClO₄)₂·6H₂O and Fe(ClO₄)₃·6H₂O with the tetradentate N₂O₂-donor Schiff bases *N,N'*-bis(salicylidene)-*ortho*-phenylenediamine and *N,N'*-bis(salicylidene)ethylenediamine (H₂salophen and H₂salen, where 2 Hs represent the two dissociable phenolic protons), respectively and the bridging ligand 4,4'-bipyridine (bipy) in presence of triethyl amine in methanol under ambient conditions produce one dimensional coordination polymers {[Mn(salophen)(μ-bipy)]ClO₄}_n (**1**) and {[Fe(salen)(μ-bipy)]ClO₄}_n (**2**) in ~60% yields. Both complexes have been characterized by elemental analysis and spectroscopic (IR and DR) measurements. The linear polymeric structures of **1** and **2** have been confirmed by single-crystal X-ray crystallography. The metal centres in these polymers are in distorted octahedral N₄O₂ coordination spheres. Each of the two dibasic tetradentate ligands (salophen²⁻ and salen²⁻) forms an ONNO square-plane around the metal centre, while the two axial coordination sites are occupied by N-atoms of the two bridging bipy ligands. Variable temperature magnetic susceptibility measurements reveal the high-spin configuration of manganese(III) and iron(III) and Curie paramagnetic behaviour of each of the two coordination polymers.

Keywords. Manganese(III); Iron(III); Schiff bases; 4,4'-bipyridine; Coordination polymers; Crystal structures; Physical properties.

1. Introduction

Since the first classification of infinite linear inorganic chain compounds as coordination polymers in 1964,¹ the design and synthesis of polymeric coordination compounds have attracted immense attention due to their interesting solid-state assembly patterns and the consequent electronic, optical and magnetic properties.^{2–11} The network structures and the physical properties of these compounds have led to their applications in a wide variety of research areas such as gas absorption, separation and storage; molecule-based conductors, magnets and sensors; nonlinear optical materials and catalysis.^{6–11} As a result, there is a constant effort for new coordination polymers having potential for use as functional materials and

efficient catalysts. We have been working on structural aspects and catalytic applications of coordination polymers involving some 3d metal ions for quite some time.^{12–14} Herein, we report two analogous one-dimensional coordination polymers of manganese(III) and iron(III) having the formulas {[Mn(salophen)(μ-bipy)]ClO₄}_n (**1**) and {[Fe(salen)(μ-bipy)]ClO₄}_n (**2**) assembled from square-planar N₂O₂ coordination geometry forming Schiff bases *N,N'*-bis(salicylidene)-*ortho*-phenylenediamine (H₂salophen) and *N,N'*-bis(salicylidene)ethylenediamine (H₂salen), respectively and the bridging ligand 4,4'-bipyridine (bipy) (Figure 1). In the following account, syntheses, single-crystal X-ray structures and the physical properties of **1** and **2** have been described.

*For correspondence

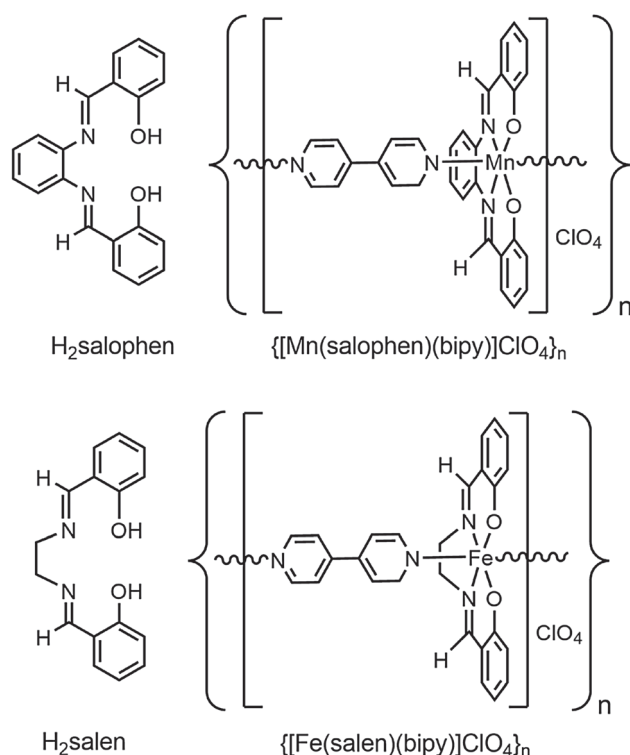


Figure 1. Chemical structure diagrams of the teradentate Schiff bases and the corresponding one-dimensional manganese(III) and iron(III) coordination polymers.

2. Experimental

2.1 Materials

The Schiff bases H_2salen and $H_2salophen$ were prepared from two-mole equivalents of salicylaldehyde and one mole equivalent of ethylene diamine and *ortho*-phenylenediamine, respectively in methanol by following a reported procedure.¹⁵ All other chemicals used in this work were of analytical grade available commercially and were used as received without any further purification. Solvents used were purified by standard methods.¹⁶

2.2 Physical measurements

Elemental (CHN) analyses were performed with the help of a Thermo Finnigan Flash EA1112 series elemental analyser. A Quantum Design SQUID-VSM instrument was used for solid-state variable temperature magnetic susceptibility measurements. The infrared spectra were recorded in ATR mode on a Thermo Scientific Nicolet iS5 FT-IR spectrophotometer. The electronic spectra were recorded in the solid-state diffuse-reflectance spectroscopy (DRS)

mode with the help of a Shimadzu UV-2600 spectrophotometer equipped with an integrating sphere.

2.3 Synthesis of $\{[Mn(salophen)(\mu-bipy)]ClO_4\}_n$ (**1**)

To a suspension of $H_2salophen$ (95 mg, 0.3 mmol) in 10 mL of methanol NEt_3 (60 mg, 0.6 mmol) and 4,4'-bipyridine (bipy) (47 mg, 0.3 mmol) were added and stirred for 10 min. To the resulting mixture a methanol solution (10 mL) of $Mn(ClO_4)_2 \cdot 6H_2O$ (110 mg, 0.3 mmol) was added and stirred in the air at room temperature (298 K) for 2 h. The brown solution obtained was filtered and the filtrate was kept for slow evaporation. The dark crystalline material separated in about 7–10 days was collected by filtration and dried in vacuum. Yield: 120 mg (64%). Anal. Calcd for $C_{30}H_{22}N_4O_6ClMn$: C, 57.66; H, 3.55; N, 8.97. Found: C, 57.62; H, 3.56; N, 8.91. Selected IR bands: ν (cm^{-1}) = 1599 (azomethine-CN), 1064 and 621 (ClO_4^-). UV-Vis (diffuse reflectance) bands: λ_{max} (nm) = 570^{sh}, 450^{sh}, 350, 252.

2.4 Synthesis of $\{[Fe(salen)(\mu-bipy)]ClO_4\}_n$ (**2**)

The iron(III) coordination polymer was also synthesized in methanolic medium by using H_2salen , NEt_3 , 4,4'-bipyridine (bipy) and $Fe(ClO_4)_3 \cdot 6H_2O$ in the same mole ratio and the same procedure as described for **1**. Yield: 105 mg (60%). Anal. Calcd for $C_{26}H_{22}N_4O_6ClFe$: C, 54.05; H, 3.84; N, 9.70. Found: C, 54.15; H, 3.86; N, 9.62. Selected IR bands: ν (cm^{-1}) = 1617 (azomethine-CN), 1083 and 618 (ClO_4^-). UV-Vis (diffuse reflectance) bands: λ_{max} (nm) = 580^{sh}, 442, 345, 248.

2.5 X-ray crystallography

A single crystal of $\{[Mn(salophen)(\mu-bipy)]ClO_4\}_n$ (**1**) suitable for X-ray data collection was collected from the crystalline material obtained from its synthesis reaction mixture. On the other hand, X-ray quality crystals of $\{[Fe(salen)(\mu-bipy)]ClO_4\}_n$ (**2**) were grown by slow evaporation of its solution in acetonitrile. Complex **1** crystallized as it is without any solvent molecule, while complex **2** formed an acetonitrile solvate **2**· CH_3CN . X-ray intensity data for both crystals were collected at 298 K on a Bruker D8 QUEST diffractometer equipped with a PHOTON 100 CMOS area detector and an INCOATEC microfocus source for graphite-monochromated Mo $K\alpha$ radiation ($\lambda =$

0.71073 Å). Data collection and reduction were performed with the help of APEX3 package.¹⁷ Absorption corrections were applied using the SADABS program.¹⁸ Each of the two structures was solved by direct method and refined on F^2 by full-matrix least-squares procedures. All non-hydrogen atoms of **1** and except for the non-hydrogen atoms of the two half-occupancy CH₃CN molecules, which were refined isotropically, the remaining non-hydrogen atoms of **2**·CH₃CN were refined with anisotropic thermal parameters. All hydrogen atoms of both structures were included in the structure factor calculations at idealized positions by using a riding model. The SHELX-97 programs¹⁹ available in the WinGX package²⁰ were used for structure solution and refinement. The structural illustrations were prepared using the Mercury package.²¹ Selected crystal data and refinement summary for both structures are listed in Table 1.

3. Results and Discussion

3.1 Synthesis and characterization

{[Mn(salophen)(μ-bipy)]ClO₄]_n (**1**) and {[Fe(salen)(μ-bipy)]ClO₄]_n (**2**) were synthesized in decent yields (64 and 60%, respectively) by reacting hexahydrated manganese(II) and iron(III) perchlorates,

the corresponding Schiff bases H₂salophen and H₂salen, 4,4'-bipyridine and triethylamine in 1:1:1:2 mole ratio in methanol at room temperature (300 K) under aerobic conditions. Both **1** and **2** are brown in colour. The elemental (CHN) analysis data of the two compounds are in good agreement with their molecular formulas. In the solid state, room temperature (300 K) magnetic moments of the repetitive mononuclear units are 4.61 and 6.02 μ_B for **1** and **2**, respectively. These values are close to the spin-only magnetic moments of 4.89 and 5.92 μ_B calculated for S = 2 and S = 5/2 spin states for the manganese(III) and iron(III) centres in **1** and **2**, respectively. In the case of **1**, it is very likely that the oxygen in air oxidized the manganese centre from bivalent state to the trivalent state during its synthesis from manganese(II) perchlorate under aerobic conditions.

3.2 X-ray structures

The structures of **1** and **2**·CH₃CN were solved in the space groups $P2_1/c$ and $P\bar{1}$, respectively. The asymmetric unit of **1** contains two repetitive units of the polymer, while that of **2**·CH₃CN contains one repetitive unit of the polymer and two half occupancy acetonitrile molecules. In both coordination polymers, the perchlorate ions are somewhat close to the metal coordinated polarized azomethine C–H groups

Table 1. Selected crystal data and structure refinement summary.

Complex	1	2 ·CH ₃ CN
Chemical formula	C ₃₀ H ₂₂ N ₄ O ₆ ClMn	C ₂₈ H ₂₅ N ₅ O ₆ ClFe
Formula weight	624.91	618.83
Crystal system	Monoclinic	Triclinic
Space group	$P2_1/c$	$P\bar{1}$
<i>a</i> (Å)	11.7703(5)	9.6938(18)
<i>b</i> (Å)	30.1432(16)	11.533(3)
<i>c</i> (Å)	16.4637(8)	15.084(3)
α (°)	90	102.352(13)
β (°)	99.697(2)	102.883(12)
γ (°)	90	105.925(13)
Volume (Å ³)	5757.8(5)	1511.2(5)
Z	8	2
ρ (g cm ⁻³)	1.442	1.360
μ (mm ⁻¹)	0.602	0.635
Reflections collected	208861	49255
Reflections unique	10099	5285
Reflections [$I \geq 2\sigma(I)$]	8068	3800
Data / restr. / param.	10099/0/757	5285/0/369
R1, wR2 [$I \geq 2\sigma(I)$]	0.0648, 0.1945	0.0950, 0.2421
R1, wR2 [all data]	0.0813, 0.2063	0.1283, 0.2594
GoF on F^2	1.062	1.095
Max./Min. $\Delta\rho$ (e Å ⁻³)	1.698/−0.688	1.222/−0.586

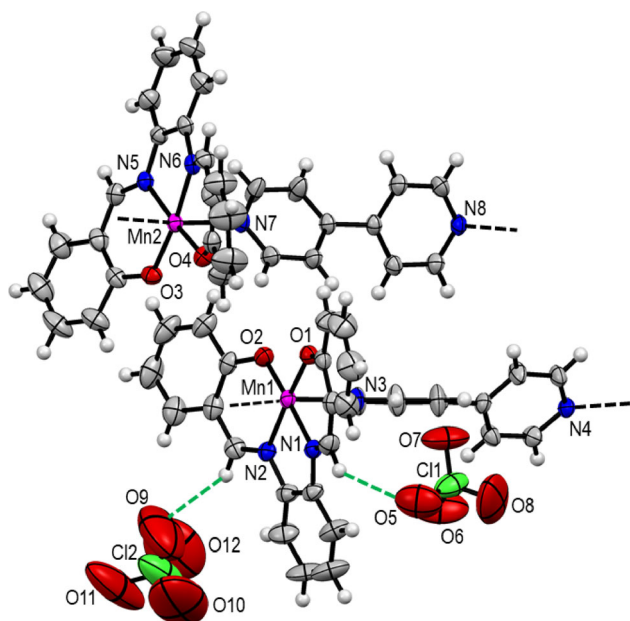


Figure 2. The asymmetric unit of **1** with the atom labelling scheme. Thermal ellipsoids of all non-hydrogen atoms are drawn at the 50% probability level. For clarity only the non-carbon atoms are labelled.

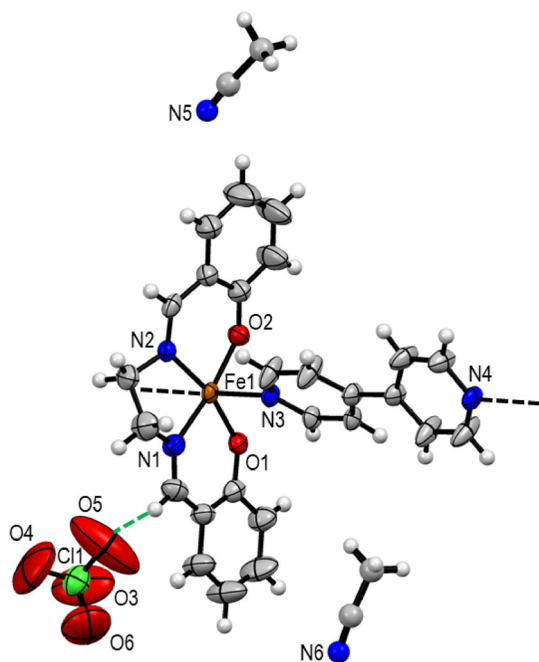


Figure 3. The asymmetric unit of **2**·CH₃CN with the atom labelling scheme. Thermal ellipsoids of all non-hydrogen atoms except for those of the two half-occupancy CH₃CN molecules are drawn at the 50% probability level. For clarity the carbon atoms are not labelled.

indicating hydrogen bonding interactions. The shortest C...O distances and the corresponding C–H...O angles are in the ranges 3.360(14)–3.618(16) Å and

123–163°, respectively. However, no significant close contact could be detected for the two half-occupancy acetonitrile molecules with the complex cation or perchlorate ion in **2**·CH₃CN. The structures of the asymmetric units of **1** and **2**·CH₃CN are illustrated in Figures 2 and 3, respectively. Metal centred geometric parameters of both are listed in Table 2. In the asymmetric unit of **1**, the bond lengths and angles associated with the manganese centres of the two repetitive cations are very similar. In each of [Mn(salophen)(μ-bipy)]⁺ and [Fe(salen)(μ-bipy)]⁺, the metal ion is in a distorted octahedral N₄O₂ coordination sphere assembled by the N₂O₂-donor Schiff base ligand and two N-atoms of the two bridging 4,4'-bipyridine molecules. The tetradentate Schiff base forms an ONNO square-plane around the metal centre. There is no deviation of the metal ion from this square-plane. The rms deviations from the mean plane constituted by the metal centre and the four coordinating atoms are about 0.03 and 0.07 Å for **1** and **2**, respectively. The N-atoms of two symmetry related 4,4'-bipyridine molecules satisfy the two axial positions of the metal centre in each of the planar {Mn(salophen)}⁺ and {Fe(salen)}⁺ units. As a result infinite linear chains of [Mn(salophen)(μ-bipy)]⁺ and [Fe(salen)(μ-bipy)]⁺ are formed in the crystal lattices of **1** and **2**·CH₃CN, respectively (Figure 4). The bridging 4,4'-bipyridine moieties are twisted in both complexes. The twisting is relatively more in **1** than in **2**. In the asymmetric unit of **1**, the dihedral angles between the two pyridine rings are 49.7(2)° and 37.8(2)° in the first and the second [Mn(salophen)(μ-bipy)]⁺ units, respectively, whereas, in [Fe(salen)(μ-bipy)]⁺, the dihedral angle is 28.2(4)°. The metal to coordinating atom distances observed for [Mn(salophen)(μ-bipy)]⁺ and [Fe(salen)(μ-bipy)]⁺ are comparable with bond lengths reported for manganese(III) and iron(III) complexes, respectively, having similar coordinating atoms.^{22–25} Bond valence sum calculations were also carried out using the EXPO2014²⁶ software for further confirmation of the oxidation states. The values obtained are 3.21 and 3.19 for the two metal centres of the two [Mn(salophen)(μ-bipy)]⁺ units present in the asymmetric unit of **1**, whereas that is 2.99 for iron in [Fe(salen)(μ-bipy)]⁺ present in the asymmetric unit of **2**·CH₃CN.

3.3 Spectroscopic properties

Infrared spectra of **1** and **2** were recorded in the range 4000–400 cm^{−1}. Both spectra display a large number of bands of various intensities (Figure 5). No attempt

Table 2. Selected bond lengths (Å) and angles (°) for **1** and **2**·CH₃CN.

[[Mn(salophen)(μ-bipy)]ClO ₄] _n (1)			
Mn(1)–O(1)	1.871(3)	Mn(2)–O(3)	1.886(3)
Mn(1)–O(2)	1.879(3)	Mn(2)–O(4)	1.865(3)
Mn(1)–N(1)	1.984(3)	Mn(2)–N(5)	1.977(3)
Mn(1)–N(2)	1.983(3)	Mn(2)–N(6)	1.994(3)
Mn(1)–N(3)	2.315(3)	Mn(2)–N(7)	2.334(3)
Mn(1)–N(4') ^a	2.396(3)	Mn(2)–N(8') ^a	2.390(3)
O(1)–Mn(1)–O(2)	95.05(13)	O(3)–Mn(2)–O(4)	94.10(12)
O(1)–Mn(1)–N(1)	91.91(13)	O(3)–Mn(2)–N(5)	91.80(13)
O(1)–Mn(1)–N(2)	173.09(14)	O(3)–Mn(2)–N(6)	172.84(13)
O(1)–Mn(1)–N(3)	90.74(13)	O(3)–Mn(2)–N(7)	91.72(12)
O(1)–Mn(1)–N(4') ^a	89.19(12)	O(3)–Mn(2)–N(8') ^a	89.32(12)
O(2)–Mn(1)–N(1)	172.87(13)	O(4)–Mn(2)–N(5)	172.81(13)
O(2)–Mn(1)–N(2)	91.41(13)	O(4)–Mn(2)–N(6)	92.69(13)
O(2)–Mn(1)–N(3)	92.10(12)	O(4)–Mn(2)–N(7)	94.21(12)
O(2)–Mn(1)–N(4') ^a	91.52(12)	O(4)–Mn(2)–N(8') ^a	88.72(12)
N(1)–Mn(1)–N(2)	81.70(14)	N(5)–Mn(2)–N(6)	81.27(13)
N(1)–Mn(1)–N(3)	89.32(12)	N(5)–Mn(2)–N(7)	89.73(12)
N(1)–Mn(1)–N(4') ^a	87.06(12)	N(5)–Mn(2)–N(8') ^a	87.23(12)
N(2)–Mn(1)–N(3)	86.57(13)	N(6)–Mn(2)–N(7)	90.02(12)
N(2)–Mn(1)–N(4') ^a	93.09(12)	N(6)–Mn(2)–N(8') ^a	88.59(12)
N(3)–Mn(1)–N(4') ^a	176.38(12)	N(7)–Mn(2)–N(8') ^a	176.82(12)
[[Fe(salen)(μ-bipy)]ClO ₄] _n ·CH ₃ CN (2 ·CH ₃ CN)			
Fe(1)–O(1)	1.871(4)	Fe(1)–O(2)	1.906(4)
Fe(1)–N(1)	2.123(6)	Fe(1)–N(2)	2.097(5)
Fe(1)–N(3)	2.231(5)	Fe(1)–N(4') ^b	2.232(5)
O(1)–Fe(1)–O(2)	105.9(2)	O(1)–Fe(1)–N(1)	88.7(2)
O(1)–Fe(1)–N(2)	165.0(2)	O(1)–Fe(1)–N(3)	90.24(19)
O(1)–Fe(1)–N(4') ^b	88.80(19)	O(2)–Fe(1)–N(1)	164.5(2)
O(2)–Fe(1)–N(2)	89.0(2)	O(2)–Fe(1)–N(3)	86.6(2)
O(2)–Fe(1)–N(4') ^b	90.8(2)	N(1)–Fe(1)–N(2)	76.8(2)
N(1)–Fe(1)–N(3)	88.1(2)	N(1)–Fe(1)–N(4') ^b	94.8(2)
N(2)–Fe(1)–N(3)	92.9(2)	N(2)–Fe(1)–N(4') ^b	88.8(2)
N(3)–Fe(1)–N(4') ^b	176.9(2)		

Symmetry transformations used to generate equivalent atoms: ^a x + 1, y, z. ^b x, y + 1, z.

was made to assign all the bands except for a selected few. The free Schiff bases H₂salophen and H₂salen are reported to show the phenolic-OH stretches as a broad band centred at 3450 and 3318 cm⁻¹, respectively.^{27,28} As expected no such band is present in the spectra of **1** and **2** due to the deprotonation of the phenolic-OH groups in both compounds. A sharp and strong band observed at 1599 cm⁻¹ for **1** is assigned to the azomethine C=N group. This C=N stretching band in **1** is about 11 cm⁻¹ lower than that in the free H₂salophen.²⁷ Similarly **2** displays a sharp and strong band at 1617 cm⁻¹, which is about 15 cm⁻¹ lower than that in the corresponding free Schiff base.²⁸ The shift of the C=N stretch to lower energy in each of the two polymers is consistent with the coordination of the azomethine-N atom to the metal centre. The presence of the perchlorate ion in **1** and **2** is indicated by a very strong and broad band centred at ~1070 cm⁻¹ and a sharp strong band at ~620 cm⁻¹.

The optical features of **1** and **2** were determined by UV–Vis diffuse reflectance spectroscopy using BaSO₄ as the reference. The spectral profiles are very similar except for some shift in the band positions and variations in their relative intensities (Figure 6). Both compounds display a weak shoulder at ~575 nm, followed by a relatively strong absorption at ~455 nm and two very strong absorptions at ~348 and ~250 nm. The electronic spectra of H₂salophen and H₂salen are known to show three strong absorptions in the range 368–214 nm.^{27,29} A ligand centred absorption band of the 4,4'-bipyridine has been reported to be observed at 363 nm.³⁰ Thus, for **1** and **2**, the two bands in the ultraviolet region (~348 and ~250 nm) are assigned to ligand centred transitions and the two visible region absorptions (~575 and ~455 nm) are attributed to ligand-to-metal charge transfer (LMCT) transitions. Previously reported manganese(III) and iron(III) complexes with salen type ligands display LMCT bands in the comparable wavelength range.^{24,25,31}

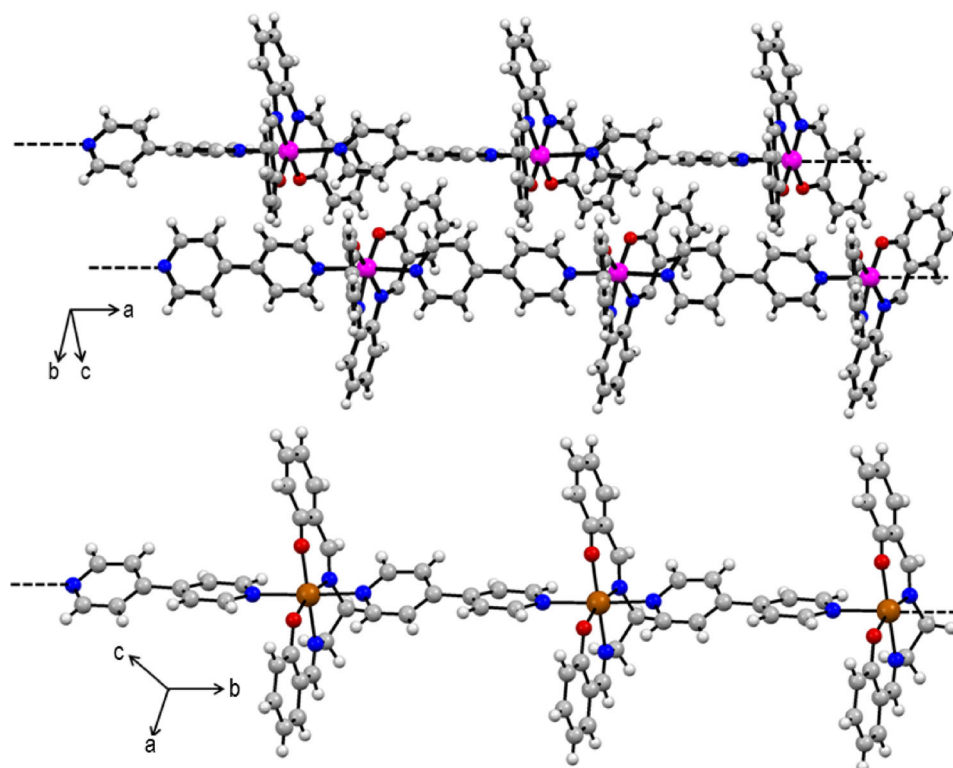


Figure 4. One-dimensional linear structures of $\{[\text{Mn}(\text{salophen})(\mu\text{-bipy})]^+\}_n$ (top) and $\{[\text{Fe}(\text{salen})(\mu\text{-bipy})]^+\}_n$ (bottom).

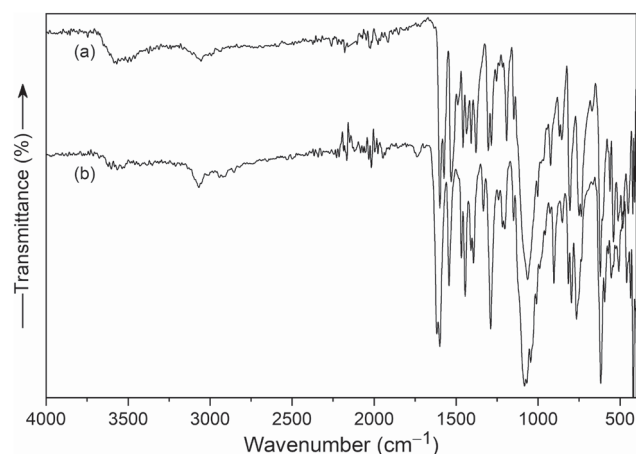


Figure 5. Infrared spectra of (a) $\{[\text{Mn}(\text{salophen})(\mu\text{-bipy})]\text{ClO}_4\}_n$ (**1**) and (b) $\{[\text{Fe}(\text{salen})(\mu\text{-bipy})]\text{ClO}_4\}_n$ (**2**).

3.4 Magnetic properties

The magnetic properties of **1** and **2** were investigated by variable temperature magnetic susceptibility measurements with their powdered samples in the temperature range 5–300 K at a constant magnetic field of 1000 Oe. The effective magnetic moment (μ_{eff}) of the repetitive unit of **1** is found to be $4.61 \mu_{\text{B}}$ at 300 K, which is somewhat lower than the calculated spin-only value

($4.89 \mu_{\text{B}}$) of high-spin manganese(III) ($S = 2$). There is essentially no change in the magnetic moment with lowering of temperature down to 65 K, where μ_{eff} is $4.59 \mu_{\text{B}}$ (Figure 7). On further lowering the temperature it increases slightly and becomes $4.65 \mu_{\text{B}}$ at 20 K and then decreases rapidly to a value of $4.34 \mu_{\text{B}}$. In case of the repetitive unit of **2**, the μ_{eff} is $6.02 \mu_{\text{B}}$ at 300 K, which is very close to the spin-only value ($5.92 \mu_{\text{B}}$) of high-spin iron(III) ($S = 5/2$). With lowering of temperature the μ_{eff} decreases and reaches the value of $5.91 \mu_{\text{B}}$ at 50 K and then increases slightly to $5.94 \mu_{\text{B}}$ at 20 K (Figure 7). Below 20 K the μ_{eff} decreases rather sharply to a value of $5.68 \mu_{\text{B}}$ at 5 K. The extents of overall decrease of the μ_{eff} values due to lowering of temperature from 300 to 5 K are 0.27 and $0.34 \mu_{\text{B}}$ for **1** and **2**, respectively. Thus it appears that there is no significant spin-spin interaction in either of the two coordination polymers. The inverse molar magnetic susceptibility values of the repetitive units of **1** and **2** are plotted against temperature (Figure 7). A near perfect linear plot has been obtained for each of **1** and **2**. In both cases, the data were fitted using the expression for the Curie–Weiss law. The Curie (C in $\text{cm}^3 \text{K mol}^{-1}$) and Weiss (θ in K) constants obtained are 2.65 and -0.40 for **1** and 4.55 and -1.87 for **2**. The linear plots and the intercepts very close to the origin indicate the Curie paramagnetic behaviour of

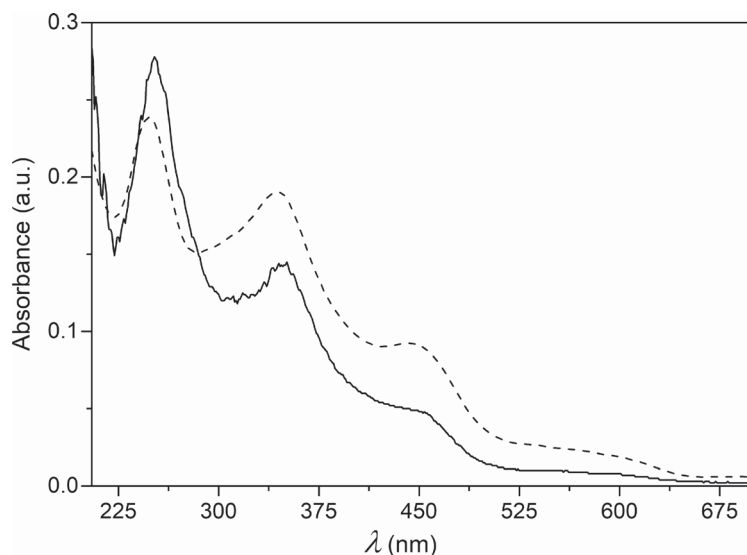


Figure 6. Diffuse reflectance spectra of $\{[\text{Mn}(\text{salophen})(\mu\text{-bipy})]\text{ClO}_4\}_n$ (**1**) (solid trace) and $\{[\text{Fe}(\text{salen})(\mu\text{-bipy})]\text{ClO}_4\}_n$ (**2**) (dashed trace).

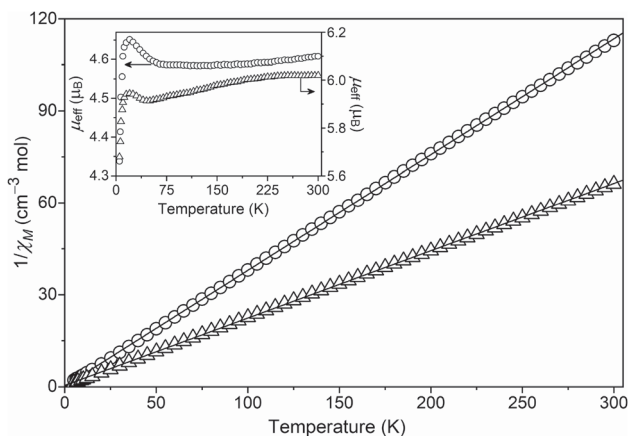


Figure 7. Inverse molar magnetic susceptibility as a function of temperature for $\{[\text{Mn}(\text{salophen})(\mu\text{-bipy})]\text{ClO}_4\}_n$ (**1**) (O) and $\{[\text{Fe}(\text{salen})(\mu\text{-bipy})]\text{ClO}_4\}_n$ (**2**) (Δ). The straight lines represent linear least-squares fits. Inset: Variation of effective magnetic moments with temperature for $\{[\text{Mn}(\text{salophen})(\mu\text{-bipy})]\text{ClO}_4\}_n$ (**1**) (O) and $\{[\text{Fe}(\text{salen})(\mu\text{-bipy})]\text{ClO}_4\}_n$ (**2**) (Δ).

both coordination polymers. The μ_{eff} calculated from the above mentioned values of C are 4.60 and 6.03 μ_{B} for **1** and **2**, respectively. Generally very weak or no spin-spin interactions are reported for 4,4'-bipyridine bridged complexes.^{23,32} A possible explanation proposed for such magnetic behaviour is as follows.³² The single bond character of the C–C bond (1.477(5) and 1.491(5) Å in **1** and 1.482(9) Å in **2**) between the two pyridine rings of the bridging 4,4'-bipyridine allows unhindered twisting of the two pyridine rings around this C–C bond (*vide supra*) and therefore prevents the super-exchange pathway *via* the pyridine ring π -electrons for effective spin-spin interaction between the bridged metal ions.

4. Conclusions

Syntheses and characterization of two one-dimensional coordination polymers of formulas $\{[\text{Mn}(\text{salophen})(\mu\text{-bipy})]\text{ClO}_4\}_n$ (**1**) and $\{[\text{Fe}(\text{salen})(\mu\text{-bipy})]\text{ClO}_4\}_n$ (**2**) with N_2O_2 -donor Schiff base ligands (salophen²⁻ and salen²⁻) and 4,4'-bipyridine (bipy) are reported. Structures of both coordination polymers were determined by single crystal X-ray crystallography. In each structure, the twisted 4,4'-bipyridine molecules act as bridges by occupying the axial coordination sites of the metal ions of the planar $\{\text{M}(\text{salophen}/\text{salen})\}^+$ units and assemble the one-dimensional linear structures of $\{[\text{M}(\text{salophen}/\text{salen})(\mu\text{-bipy})]\}^+$. Microanalytical and the solid state infrared and electronic spectroscopic characteristics of both polymeric compounds are consistent with their structures. Variable temperature magnetic susceptibility studies revealed the $S = 2$ and $5/2$ spin states of the metal ions in **1** and **2**, respectively and their Curie paramagnetic character due to twisting of the bridging 4,4'-bipyridine, which does not allow any super-exchange induced spin-spin interaction between the metal ions.

Supplementary Information (SI)

CCDC 2077457 and 2077458 contain the supplementary crystallographic data for **1** and **2-CH₃CN**, respectively. These data can be obtained free of charge via www.ccdc.cam.ac.uk/data_request/cif, by e-mailing to data_request@ccdc.cam.ac.uk or by contacting The Cambridge Crystallographic Data Centre, 12

Union Road, Cambridge CB2 1EZ, UK; fax: (+44)1223-336-033.

Acknowledgements

A. K. Srivastava thanks the University Grants Commission (UGC), New Delhi for a research fellowship (No. F.25-1/2014-15(BSR)/5-129/2007(BSR)). The cryomagnetic measurements were performed at the UGC-DAE Consortium for Scientific Research, Indore. Financial and infrastructural supports from the UGC (through the CAS program) and the Department of Science and Technology (DST), New Delhi (through the FIST program) are gratefully acknowledged. We thank the Ministry of Education, Government of India for financial assistance (Grant no. F11/9/2019-U3(A)) to the University of Hyderabad–Institution of Excellence.

References

- Bailar JC Jr 1964 In *Preparative Inorganic Reactions* Vol. 1 WL Jolly (Ed.) (Interscience: New York) pp. 1–25
- Murugavel R, Anantharaman G, Krishnamurthy D, Sathiyendiran M and Walawalkar MG 2000 Extended metal–organic solids based on benzenepolycarboxylic and aminobenzoic acids *Proc. Indian Acad. Sci. (Chem. Sci.)* **112** 273
- Rajput L, Sarkar M and Biradha K 2010 Assembling one-dimensional coordination polymers into three-dimensional architectures via hydrogen bonds *J. Chem. Sci.* **122** 707
- Dzhardimalieva GI and Uflyand IE 2017 Design and synthesis of coordination polymers with chelated units and their applications in nanomaterials science *RSC Adv.* **7** 42242
- Engel ER and Scott JL 2020 Advances in the green chemistry of coordination polymer materials *Green Chem.* **22** 3693
- Chen C-T and Suslick KS 1993 One-dimensional coordination polymers: Applications to material science *Coord. Chem. Rev.* **128** 293
- Batten SR, Neville SM and Turner DR 2009 *Coordination Polymers: Design, Analysis and Application* (Cambridge: RSC Publishing)
- Mas-Ballesté R, Gómez-Herrero J and Zamora F 2010 One-dimensional coordination polymers on surfaces: towards single molecule devices *Chem. Soc. Rev.* **39** 4220
- Leong WL and Vittal JJ 2011 One-Dimensional Coordination Polymers: Complexity and Diversity in Structures, Properties, and Applications *Chem. Rev.* **111** 688
- Loukopoulos E and Kostakis GE 2018 Review: Recent advances of one-dimensional coordination polymers as catalysts *J. Coord. Chem.* **71** 371
- Liu J-Q, Luo Z-D, Pan Y, Singh AK, Trivedi M and Kumar A 2020 Recent developments in luminescent coordination polymers: Designing strategies, sensing application and theoretical evidences *Coord. Chem. Rev.* **406** 213145
- Sangeetha NR and Pal S 2000 Dimeric and polymeric square-pyramidal copper(II) complexes containing equatorial–apical chloride or acetate bridges *Polyhedron* **19** 1593
- Das S, Maloth S and Pal S 2011 Nickel(II) Coordination Polymers – 4,4'-Bipyridine-Connected Six- and Four-fold Metal–succinate Helices and Their Corresponding Chiral and Achiral Networks *Eur. J. Inorg. Chem.* 4270
- Srivastava AK, Ghosh S and Pal S 2019 A one-dimensional polymeric mixed-valent Mn(II)Mn(III) complex with a macrocyclic compartmental ligand: Structure, properties and catecholase like activity *Polyhedron* **172** 112
- Zhou L, Feng Y, Cheng J, Sun N, Zhou X and Xiang H 2012 Simple, selective, and sensitive colorimetric and ratiometric fluorescence/phosphorescence probes for platinum(II) based on Salen-type Schiff bases *RSC Adv.* **2** 10529
- Perrin DD, Armarego WLF and Perrin DP 1983 *Purification of Laboratory Chemicals* (Oxford: Pergamon)
- APEX3: Program for Data Collection on Area Detectors, 2014 Bruker Analytical X-ray Systems Inc., Madison Wisconsin, USA
- Sheldrick GM 1997 *SADABS. Program for Area Detector Absorption Correction* (University of Göttingen: Göttingen)
- Sheldrick GM 2008 A short history of SHELX *Acta Crystallogr. Sect. A* **64** 112
- Farrugia LJ 1999 WinGX suite for small-molecule single-crystal crystallography *J. Appl. Crystallogr.* **32** 837
- Macrae F, Bruno IJ, Chisholm JA, Edgington PR, Cabe PM, Pidcock E, et al. 2008 New features for the visualization and investigation of crystal structures *J. Appl. Crystallogr.* **41** 466
- Zhou Y-X, Zheng X-F, Han D, Zhang H-Y, Shen X-Q, Niu C-Y, et al. 2006 Syntheses and Crystal Structures of Fe(III) and Mn(III) Complexes with Salen Ligands: [Fe(salen)Cl]·CH₃CN and [Mn(salen)(SCN)(CH₃OH)]·CH₃CN *Synth. React. Inorg. Met.-Org. Nano-Met. Chem.* **36** 693
- Deawati Y, Onggo D, Mulyani I, Hastiawan I, Kurnia D, Lönnecke P, et al. 2018 Synthesis, crystal structures, and superoxide dismutase activity of two new multinuclear manganese(III)-salen-4,4'-bipyridine complexes *Inorg. Chim. Acta* **482** 353
- Shova S, Vlad A, Cazacu M, Krzystek J, Bucinsky L, Breza M, et al. 2017 A five-coordinate manganese(III) complex of a salen type ligand with a positive axial anisotropy parameter *D Dalton Trans.* **46** 11817
- Cozzolino M, Leo V, Tedesco C, Mazzeo M and Lamberti M 2018 Salen, salan and salalen iron(III) complexes as catalysts for CO₂/epoxide reactions and ROP of cyclic esters *Dalton Trans.* **47** 13229
- Altomare A, Cuocci C, Giacovazzo C, Moliterni A, Rizzi R, Corriero N and Falcicchio A 2013 EXPO2013: a kit of tools for phasing crystal structures from powder data *J. Appl. Crystallogr.* **46** 1231

27. Koley MK, Sivasubramanian SC, Varghese B, Manoharan PT and Koley AP 2012 A paramagnetic octahedral trans-dihydroxy chromium(IV) complex with dianionic tetradentate Schiff base salophen and crystal structure of its *trans*-diisothiocyanato analog *J. Coord. Chem.* **65** 3623
28. Hu X-M, Xue L-W, Zhao G-Q and Yang W-C 2015 Synthesis, Crystal Structure and Antimicrobial Activity of a Hetero Trinuclear Manganese(III)-Iron(II) Complex Derived from *N,N'*-Bis(5-methylsalicylidene)-1,2-diaminoethane *Bull. Chem. Soc. Ethiop.* **29** 407
29. Gao T, Yang Y, Sun W-B, Li G-M, Hou G-F, Yan PF, et al. 2013 Syntheses, structure and near-infrared (NIR) luminescence of Er₂, Yb₂, ErYb of homodinuclear and heterodinuclear lanthanide(III) complexes based on salen ligand *CrystEngComm* **15** 6213
30. Xiu-min S, Hai-yan W, Yan-bing L, Jing-xiu Y, Lei C, Ge H, et al. 2010 Spectroscopic studies on Co(II), Ni(II), Zn(II) complexes with 4,4'-bipyridine *Chem. Res. Chin. Univ.* **26** 1011
31. Kurahashi T and Fujii H 2012 Comparative Spectroscopic Studies of Iron(III) and Manganese(III) Salen Complexes Having a Weakly Coordinating Triflate Axial Ligand *Bull. Chem. Soc. Jpn.* **85** 940
32. Li M-X, Xie G-Y, Gu Y-D, Chen J and Zheng P-J 1995 Synthesis, characterization and magnetic properties of one-dimensional 4,4'-bipyridine bridged manganese(II) complex: crystal structure of [Mn(μ -4,4'-bipy)(4,4'-bipy)(NCS)₂(H₂O)₂]_n *Polyhedron* **14** 1235